Analytical and Monte-Carlo modeling of Multi-Parallel Slit and Knife-Edge Slit Prompt Gamma Cameras

E. Testa[1], B.F.B. Huisman[1,2], D. Dauvergne[3], J. M. Létang[2], D. Sarrut[3]

[1]Université de Lyon, Université Claude Bernard Lyon 1, CNRS/IN2P3, Institut de Physique Nucléaire de Lyon, 69622 Villeurbanne, France, [2]CREATIS, Université de Lyon; CNRS UMR5220; INSERM U1044; INSA-Lyon; Université Lyon 1; Centre Léon Bérard, Lyon, France, [3]Université Grenoble Alpes, Laboratoire de Physique Subatomique et de Cosmologie, CNRS/IN2P3, Grenoble, France

1. Introduction

Ion-range verification during hadrontherapy

- Major challenge to fully take benefit from ion beam ballistic properties
- Main imaging modalities under study: prompt gammas (PG) detection [1] with non-imaging systems (such as PG Timing, PG Spectroscopy and PG Peak Integral) and imaging systems, namely physically-collimated or electronically collimated cameras (Compton cameras)

PG collimated cameras

- 2 main collimator configurations: Multi-Parallel Slit (MPS) [2] and Knife-Edge Slit (KES) collimators [3] (Figure 1)
- No theoretical considerations have been proposed for the specific 1D collimation systems developed for PG detection

2. Objectives

- Development of an analytical model (AM) of MPS and KES collimations ⇒ main intrinsic features of each collimator
- Verification of the AM by means of Monte Carlo (MC) simulations
- Comparison the MPS and KES prototypes developed by the CLaRyS collaboration [2] and IBA [3], respectively.

3. The Analytical Model of MPS and KES collimations

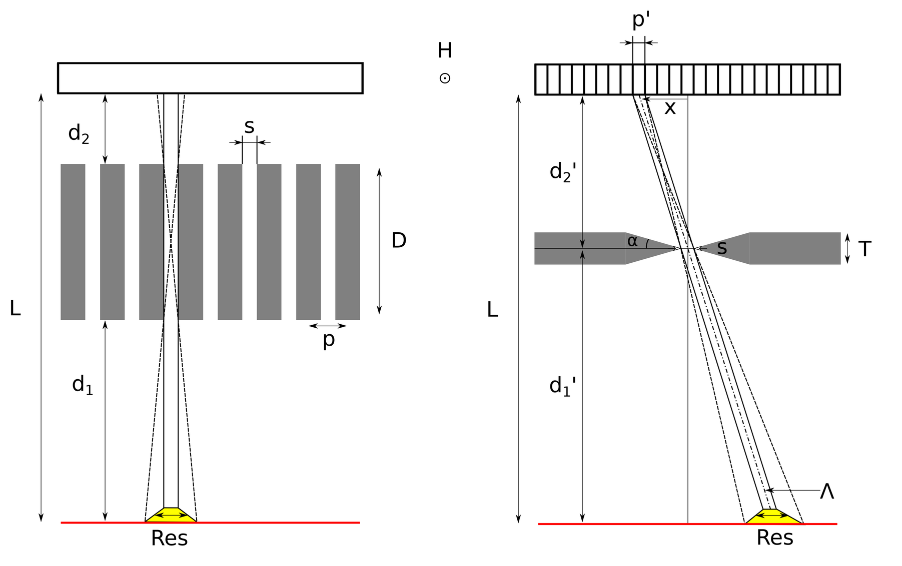

Figure 1: MPS (left) and KES (right) collimation

	MPS	KES
s_e	s	$s + \frac{\ln(2)}{\mu\ \tan(\alpha)}$
FOW	$s\left(1+\frac{d_1}{D}\right)$	$s_e\left(1+\frac{d_1'}{d_2'}\right)$
DE	$\frac{Hs}{4\pi LD}(1-f)$	$\frac{Hs_e}{4\pi Ld_2'}\left(1+\frac{x^2}{d_2'^2}\right)^{-3/2}$
T_e	$D \times f$	T

Table 1: Detection efficiencies (DE) and spatial resolution (Res=FOW) predicted by the analytical model. FOW: Fall-Off Width of the PG profile (see "Figures of merit") ; s_e: effective slit width ; T_e: Collimator effective thickness.

4. Monte Carlo simulations & PG profile analysis

- Monte Carlo simulations
  - 2-stage simulation with Gate 7.2 (Geant4 4.10.02)
  - First stage: target irradiation (QGSP_BIC_HP_EMY physics list)
    - Optimization: vpgTLE variance reduction method ⇒ gain of $\sim 10^3$ [4]
  - Second stage: photon propagation in the geometry (emlivermore physics list)
- PG profile analysis
  - Background (BKG) modeling:
    - Estimates of background counts in the detector (mainly due to secondary neutrons) are taken from [2] (MPS, 2.5×10^{-7} counts/incident proton and per 8 mm bin) and [5] (KES, 5×10^{-7} counts per primary proton per 4 mm bin) which are both based on measured data
  - Fall-Off Position (FOP): position corresponding to the half FO amplitude in the spline-fit to the PG profile
  - Fall-Off Width (FOW) : width of the PG profile fall-off, namely the FWHM of the peak resulting from the computation of the PG profile first derivative (see bottom row of Figure 3)

5. Simulated geometries

- 2 configurations (Table 2):
  - The prototypes as they are published (Figure 2)
  - The prototypes with some alterations for the Analytical Model Verification (AMV)

		AMV	PC
Absorber	MPS	Perfect	BGO
	KES		LYSO
Collimator		Perfect	Real
Energy selection	MPS	> 1 MeV	> 1 MeV
	KES		3–6 MeV
TOF selection	MPS	no TOF	TOF
	KES		no TOF
BKG		No modeling	Exp. data based
Target		No	Yes
Beam		160 MeV proton	

Table 2: AMV: Analytical Model Verification – PC: Prototypes Comparison. "Perfect" collimators and detectors: gamma full absorption. For AMV, the PG source corresponds to the PG emitted along the beam direction during the PMMA irradiation

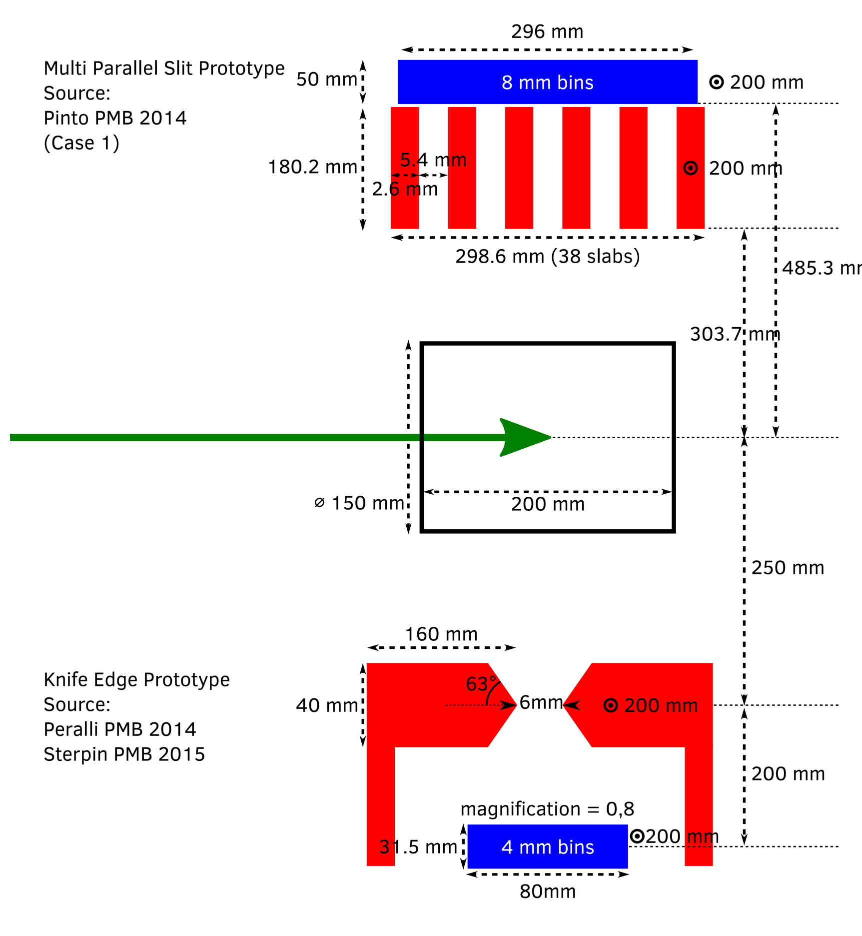

Figure 2: Prototypes representation

6. Figures of merit

- Detection efficiency (DE): #detected PG/#emitted PG in the camera Field of View
- Spatial resolution (Res) = FOW (Fall-Off Width)
- Fall-off Retrieval Precision (FRP): Standard deviation of the FOP distribution obtained with 50 MC simulation runs.

7. Results

AMV

	MPS		KES	
	AM	MC	AM	MC
FOW (mm)	14.5	16.9	13.5	13.8
DE	$\mathbf{6.66 \times 10^{-4}}$	$\mathbf{6.47 \times 10^{-4}}$	$\mathbf{1.06 \times 10^{-3}}$	$\mathbf{8.7 \times 10^{-4}}$

PG profiles detected by the prototypes

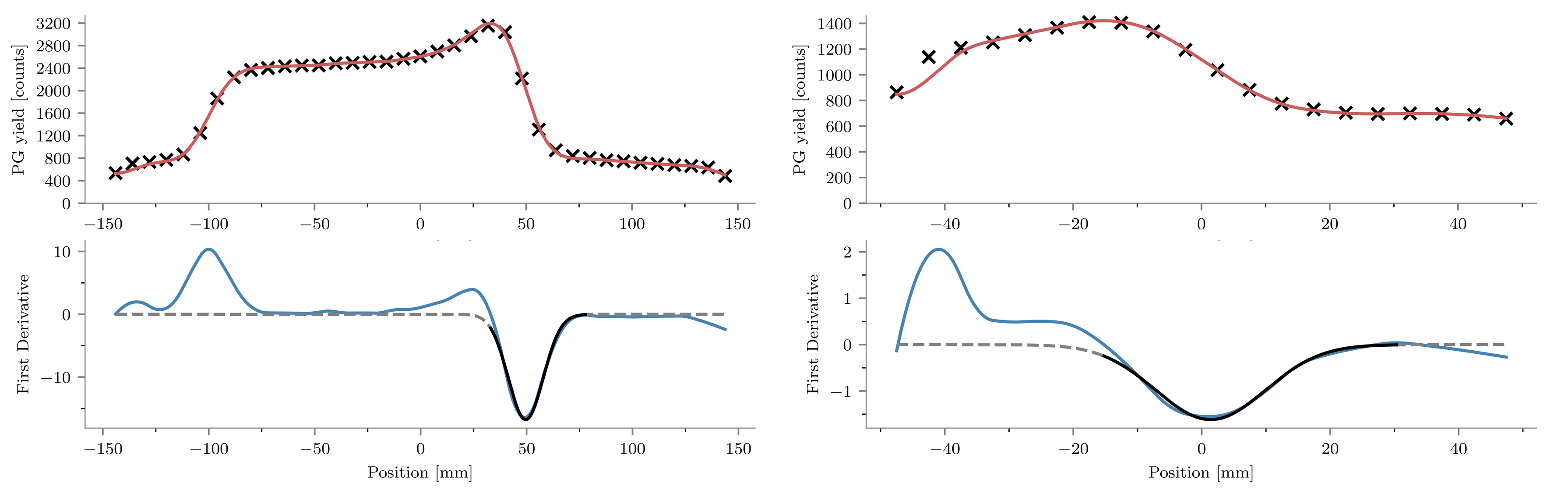

Figure 3: Top: PG profiles obtained with MPS (left) and KES (right). See column PC of Table 2 for the parameters. Bottom: first derivative of the PG profiles.

Fall-off Retrieval Precision

# protons	MPS	KES
$\mathbf{10^9}$	0.32	0.65
$\mathbf{10^8}$	1.05	1.80
$\mathbf{10^7}$	2.81	17.1

Table 3: Standard deviations (in mm) of the FOP distributions. See column PC of Table 2 for the parameters.

8. Discussion and conclusion

- Analytical Model (AM)
  - Good agreement in overall with MC
  - Striking similarities between MPS and KES performances, unlike what can be concluded from previous studies [6, 7, 8]
    - ⇒ Same DE and FOW with perfect collimators
    - ⇒ With real collimators: slightly poorer DE for MPS and FOW for KES
    - Note that the MPS prototype allows for the detection of the whole PG profile: the field of view of the MPS and KES prototypes are of 30 cm and 10 cm, respectively
- Prototypes comparison
  - PG profiles: MPS prototype with larger fall-off amplitude and lower BKG level thanks to larger energy and TOF selections, respectively
  - ⇒ Better Fall-Off Retrieval Precision (FRP) with the MPS prototype
  - Precisions in agreement with the ones published in [2] and [3]

References

[1] J. Krimmer and et al., "Prompt-gamma monitoring in hadrontherapy: A review," *NIMA*, 2017.
[2] M. Pinto and et al., "Design optimisation of a TOF-based collimated camera prototype for online hadrontherapy monitoring.," *PMB*, vol. 59, 2014.
[3] J. Smeets and et al., "Prompt gamma imaging with a slit camera for real-time range control in proton therapy," *PMB*, 2012.
[4] B. F. B. Huisman and et al., "Accelerated prompt gamma estimation for clinical proton therapy simulations," *PMB*, 2016.
[5] I. Perali and et al., "Prompt gamma imaging of proton pencil beams at clinical dose rate," *PMB*, 2014.
[6] J. Smeets and et al., "Exp. Comparison of KES and MPS Collimators for Prompt Gamma Imaging of Proton Pencil Beams," *RO*, 2016.
[7] H.-H. Lin and et al., "A comparison of two prompt gamma imaging techniques with collimator-based cameras for range verification in proton therapy," *RPC*, 2016.
[8] J. H. Park and et al., "Comparison of knife-edge and multi-slit camera for proton beam range verification by Monte Carlo simulation," *NET*, vol. 51, 2019.

Labex PRIMES ANR-11-LABX-0063.

contact: e.testa@ipnl.in2p3.fr